AGU PUBLICATIONS

JGR

Journal of Geophysical Research: Atmospheres

RESEARCH ARTICLE

10.1002/2013JD020560

Key Points:
- New methodology to analyze SSW on the tropical stratosphere
- There are differences in the SSW tropical cooling according to QBO phase
- Zero-wind line position plays an important role in SSW tropical response

Correspondence to:
M. Gómez-Escolar,
mgomezes@fis.ucm.es

Citation:
Gómez-Escolar, M., N. Calvo, D. Barriopedro, and S. Fueglistaler (2014), Tropical response to stratospheric sudden warmings and its modulation by the QBO, *J. Geophys. Res. Atmos.*, *119*, 7382–7395, doi:10.1002/2013JD020560.

Received 14 JUL 2013
Accepted 13 JAN 2014
Accepted article online 1 APR 2014
Published online 30 JUN 2014

Tropical response to stratospheric sudden warmings and its modulation by the QBO

M. Gómez-Escolar[1], N. Calvo[1], D. Barriopedro[1,2,3], and S. Fueglistaler[4]

[1]Departamento Astrofísica y Ciencias de la Atmósfera, Universidad Complutense de Madrid, Madrid, Spain, [2]Instituto de Geociencias, CSIC-UCM, Madrid, Spain, [3]Instituto Dom Luiz, Universidade de Lisboa, Portugal, [4]AOS, Department of Geosciences, Princeton University, Princeton, New Jersey, USA

Abstract Major Stratospheric Sudden Warmings (SSWs) are characterized by a reversal of the zonal mean zonal wind and an anomalous warming in the polar stratosphere that proceeds downward to the lower stratosphere. In the tropical stratosphere, a downward propagating cooling is observed. However, the strong modulation of tropical winds and temperatures by the quasi-biennial oscillation (QBO) renders accurate characterization of the tropical response to SSWs challenging. A novel metric based on temperature variations relative to the central date of the SSW using ERA-Interim data is presented. It filters most of the temperature structure related to the phase of the QBO and provides proper characterization of the SSW cooling amplitude and downward propagation tropical signal. Using this new metric, a large SSW-related cooling is detected in the tropical upper stratosphere that occurs almost simultaneously with the polar cap warming. The tropical cooling weakens as it propagates downward, reaching the lower stratosphere in a few days. Substantial differences are found in the response to SSWs depending on the QBO phase. Similar to what is observed in the polar stratosphere, tropical SSW-associated temperatures persist longer during the west QBO phase at levels above about 40 hPa, suggesting that the signal is mainly controlled by changes in the residual mean meridional circulation associated with SSWs. Conversely, in the lower stratosphere, around 50–70 hPa, enhanced cooling occurs only during QBO east phase. This behavior seems to be driven by anomalous subtropical wave breaking related to changes in the zero-wind line position with the QBO phase.

1. Introduction

Stratospheric Sudden Warmings (SSWs) are extreme events able to modify the polar cap temperature within a few days [e.g., *Andrews et al.*, 1987]. They are preceded by anomalously strong wave activity from the troposphere that propagates into the stratosphere and breaks at polar jet latitudes around 10 hPa or higher. Their dissipation decelerates the polar vortex and might even result in a reversal of the zonal wind direction from westerlies to easterlies. Previous studies have shown that the residual mean meridional circulation is affected during the life cycles of the SSWs [*Matsuno*, 1971]. Thus, the downwelling and warming over the polar cap characteristic of SSWs is accompanied by upwelling and cooling in the low latitudes of the tropical stratosphere [e.g., *Randel et al.*, 2002; *Holton et al.*, 1995; *Haynes et al.*, 1991].

In the tropics, the quasi-biennial oscillation (QBO) is a major contributor to stratospheric variability. It is a downward propagating oscillation of the zonal mean zonal winds with a period of about 28 months, driven by wave dissipation [e.g., *Baldwin et al.*, 2001, and references therein]. Its effects are not only noticeable in the tropics. The QBO modulation of the position of the zero-wind line in the subtropics also influences the polar vortex. During the east QBO phase, the polar vortex tends to weaken as more wave activity refracts to the pole [*Holton and Tan*, 1980]. Although the QBO is fairly regular, variations in the phase speed of downward propagation make difficult to filter the tropical temperature response to SSWs.

Very few studies have investigated the tropical signal associated with SSWs. *Kodera* [2006] investigated the tropical effect of nine selected events with large deceleration of the zonal mean zonal wind between 50° and 70°N. He calculated anomalies as departures from a daily climatology and to remove the part of the anomaly related to the QBO, he subtracted the 31 day mean around the central date. SSWs were found to be associated with changes in convective activity that increased near the equatorial Southern Hemisphere (10°S–Equator) and decreased in the Northern Hemisphere (5°N–15°N). On the other hand, *Taguchi* [2011] reduced the QBO signature in the tropics decomposing the fields into long- and short-term variations.

He stated that 30°S was the latitude extent of the SSW-associated cooling and upwelling signals. He also found a correlation between the strength in the tropical cooling associated with SSWs at 10 hPa and the location of wave driving: the stronger the tropical cooling, the closer the extratropical wave driving was to subtropical latitudes. Regarding SSWs differences between QBO phases, *Naito et al.* [2003] used a three-dimensional mechanistic circulation model to run parameter sweep experiments of QBO profiles in perpetual winter conditions. They found differences between west and east QBO phases in the magnitude of the SSW tropical cooling, and two time scales for the tropical and subtropical temperature responses in the stratosphere. A short-time response (days after the SSW) extended to the summer hemisphere, and a long-time response, of several weeks, was stronger in the winter hemisphere subtropics and extended down near the tropopause. Recently, *Yoshida and Yamazaki* [2011] analyzed the tropical cooling of the SSW occurred in January 2009 by decomposing the wave forcing into its tropospheric and stratospheric parts. They concluded that stratospheric wave forcing induced anomalous cooling in the stratosphere above 100 hPa; however, the cooling observed from 100 to 150 hPa was related to a change in the convective activity associated with subtropical wave dissipation at 100 hPa. Nonetheless, both pathways of tropical cooling had the same source, i.e., the increase of midlatitude wave activity in the troposphere.

Despite these previous studies, a general description of the evolution of the SSWs signal in the tropical stratosphere has not been addressed. Here we present an analysis of temperature variations in this region in response to SSWs based on reanalysis data. We focus on eliminating the QBO structure in the tropical temperature, as well as the mean annual cycle. Section 2 describes the data and the methodology employed to identify SSWs and QBO phases. Section 3 assesses and compares different methodologies aiming to remove the QBO structure from our SSW composites. A new alternative methodology to properly eliminate these QBO structures is presented in section 4, which will provide a clearer picture of the temperature changes associated with SSWs in the entire stratosphere and the differences between QBO phases. Section 5 summarizes the main results and discusses the mechanism proposed.

2. Data and Methodology

We have used daily mean data from the European Centre for Medium Range Weather Forecasts ERA-Interim reanalysis for the period from 1979 to 2012 [*Dee et al.*, 2011]. Daily mean data have been used at 2.5° × 2.5° resolution in longitude and latitude, at the original model levels in the pressure range 100 hPa–5 hPa (in ERA-Interim the model levels are located at 5.2, 6.4, 8.0, 9.9, 12.3, 15.2, 18.8, 23.3, 28.9, 35.8, 44.3, 54.6, 66.6, 80.4, and 95.7 hPa).

In addition to daily temperature and zonal mean zonal wind, daily means of the residual circulation (v^*, w^*), the Eliassen-Palm flux ($F^{(z)}$, $F^{(\phi)}$) and its divergence ($\nabla \cdot F$) have also been computed based on 6-hourly data [*Seviour et al.*, 2012], according to equations in *Andrews et al.* [1987],

$$\overline{v}^* \equiv \overline{v} - \rho_0^{-1} \left(\rho_0 \, \overline{v'\theta'} / \overline{\theta}_z \right)_z$$

$$\overline{w}^* \equiv \overline{w} + (a cos\phi)^{-1} \left(cos\phi \overline{v'\theta'} / \overline{\theta}_z \right)_\phi$$

$$F^{(\phi)} \equiv \rho_0 \, a \cos\phi \, \left(\overline{u}_z \, \overline{v'\theta'} / \overline{\theta}_z - \overline{v'u'} \right)$$

$$F^{(z)} \equiv \rho_0 \, a \cos\phi \, \left\{ \left[f - (a \cos\phi)^{-1} \left(\overline{u} \cos\phi \right)_\phi \right] \overline{v'\theta'} / \overline{\theta}_z - \overline{w'u'} \right\}$$

$$\nabla \cdot F \equiv (a \cos\phi)^{-1} \frac{\partial}{\partial \phi} (F^{(\phi)} \cos\phi) + \frac{\partial F^{(z)}}{\partial z}$$

where a is the Earth's radius, f is the Coriolis parameter, ϕ is latitude, z is log(pressure) − height, $\rho_0 = exp(-z/H)$, H is the density-scale height taken as 7000 m, θ is potential temperature, and u,v,and w are the wind in the zonal, meridional, and vertical directions, respectively. An overbar represents the zonal mean, and a prime the deviation from this mean. Subscripts represent the partial derivative.

Table 1. SSWs Dates According to CP07 Algorithm (Second Column) and Reassigned Central Dates According to the Maximum Temperature in ±30 Days (Third Column)[a]

N	Central Date Wind Reversal	New Date	QBO Phase
1	22 Feb 1979	27 Feb 1979	W
2	1 Mar 1980	1 Mar 1980	E
3	4 Mar 1981	5 Feb 1981	W
	4 Dec 1981		
4	24 Feb 1984	24 Feb 1984	
5	1 Jan 1985	1 Jan 1985	E
6	23 Jan 1987	18 Jan 1987	
7	8 Dec 1987	8 Dec 1987	
8	14 Mar 1988	12 Mar 1988	W
9	21 Feb 1989	20 Feb 1989	W
10	15 Dec 1998	17 Dec 1998	E
11	26 Feb 1999	27 Feb 1999	
12	20 Mar 2000	13 Mar 2000	W
13	11 Feb 2001	1 Feb 2001	
14	30 Dec 2001	28 Dec 2001	E
15	17 Feb 2002	19 Feb 2002	
16	18 Jan 2003	29 Dec 2002	W
17	5 Jan 2004	25 Dec 2003	E
18	21 Jan 2006	21 Jan 2006	E
19	24 Feb 2007	24 Feb 2007	W
20	22 Feb 2008	23 Feb 2008	E
21	24 Jan 2009	23 Jan 2009	W
22	9 Feb 2010	30 Jan 2010	
	24 Mar 2010		

[a]QBO phase for each SSW (fourth column). See text for details.

The methodology presented by *Charlton and Polvani* [2007] (CP07 from now on) has been applied here to identify the central dates of the major midwinter SSWs from November to March, thus detecting 24 SSWs in the 34 year period (Table 1 second column). This criterion requires a change from westerlies to easterlies at 60°N and 10 hPa (the 9.9 hPa level has been used here). The central date of the SSW is defined as the first day with easterly zonal mean zonal wind. The algorithm considers the same event when 2 days with easterly zonal mean zonal wind are not separated by at least 20 days. Final warmings are excluded by demanding a return to westerlies for at least 10 consecutive days before the end of the winter season.

Next, the evolution of temperature anomalies at 10 hPa over the polar cap has been analyzed for each of the identified events. *Taguchi* [2011] claimed that the SSW signal on the residual mean meridional circulation was better characterized when using temperature and its variance as diagnostic fields rather than the zonal mean zonal wind reversal as in CP07. Accordingly, we have identified the day with the highest polar cap average temperature (60°–90°N) within ±30 days of each SSW's central date. The day when this occurs is considered our new central date. The temperature evolutions over the polar cap within ±30 days relative to this new central date are shown in Figure 1 for each SSW (blue lines) together with CP07 dates (red dots). Further, this objective definition of the central date was subject to visual inspection. Two SSWs (March 2010 and December 1981) identified with CP07 criteria were removed from our catalog since they were not associated with a clear warming period over the polar cap. In addition, the following requirements were demanded: (1) In the cases for which the absolute maximum temperature was reached within a period of almost constant temperature, the central date was taken as the first day of that period (e.g., Figure 1, 1987/12), it did not change the SSW central date by more than 10 days relative to the absolute maximum and it only affected 6 cases; (2) when there were two relative temperature maxima, the one closest to CP07 date was chosen in 1979/2 (Figure 1). Requirements (1) and (2) were applied as long as the difference in temperature between the two dates (that of the absolute maximum and the corrected date) was smaller than 0.5 K. Table 1 (third column) lists the new SSWs central dates. In the exceptional case of March 1981 the difference between the timing of the zonal wind reversal and the occurrence of the highest temperature is 27 days, but for most of the SSWs the new central dates do not differ by more than ±10 days with respect to those of CP07. By selecting the new central dates, the SSWs temperature anomalies in the tropics (10°S-10°N, red lines) have their largest values around day 0 at 9.9 hPa (Figure 1). The evolution of the polar (blue lines) and tropical temperatures clearly shows a mirrored behavior, with opposite evolutions in temperature, and only minor differences between the timing of maximum polar cap and minimum tropical temperatures. This behavior supports our selection of central dates.

The phase of the QBO during a SSW is defined according to the average of the equatorial zonal mean zonal wind of ±30 days around the SSW central date at the model level of 44.3 hPa. A SSW is considered to occur during the east or west QBO phase (EQBO and WQBO, respectively) when the winds at 44.3 hPa are lower or higher than −5 and +5 m/s, respectively, and there are winds of opposite sign at 9.9 hPa. Due to the slow evolution of the QBO relative to the life cycle of a SSW, changing the number of days used to average the winds around the SSW central date does not affect the classification of SSWs by their QBO phase. According

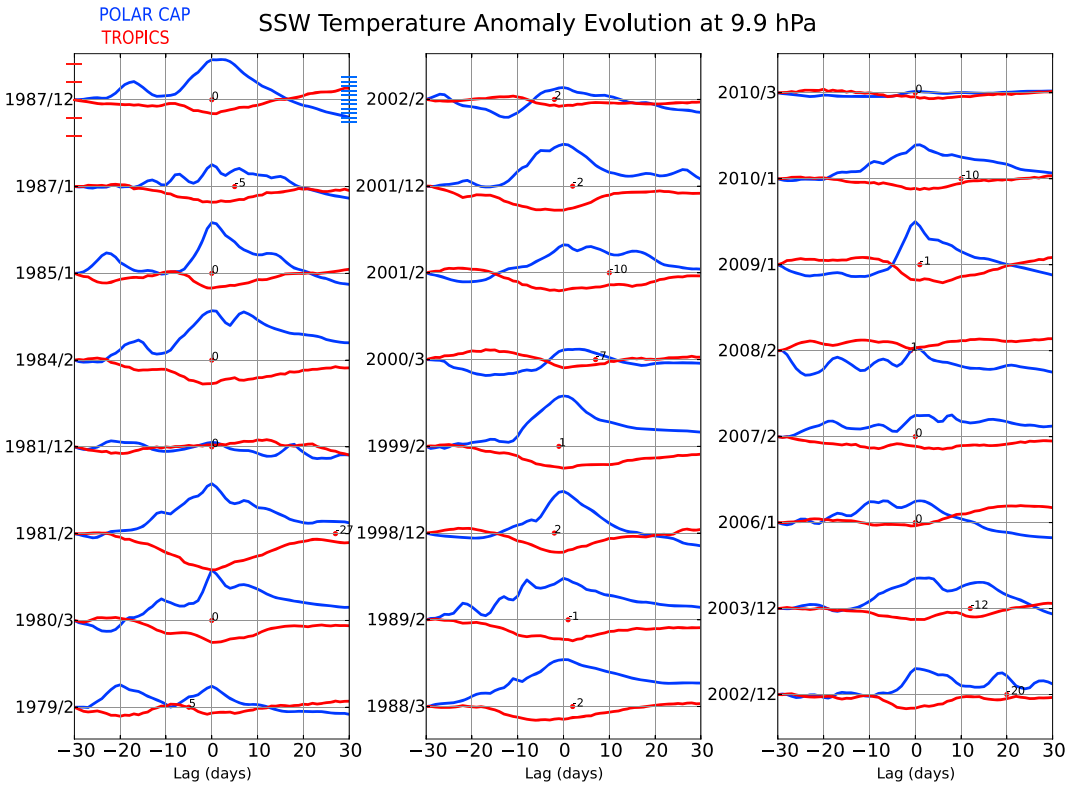

Figure 1. Polar cap (60°–90°N, blue) and tropical (10°S–10°N, red) zonal mean temperature anomaly evolution at 9.9 hPa for the −30 to +30 day period of each SSW detected in the ERA-Interim reanalysis. Red dots mark the SSW central date according to CP07 algorithm while the number indicates the lag with our new central date. Note that the temperature evolutions are plotted with reference to the value of day −30 as the start value. The tropical and polar temperature magnitudes are not comparable as they have been scaled for a better visualization with a factor of 4. Scales are indicated with temperature increments of 3 K for the upper left SSW's evolution.

to this definition, there are seven SSWs during EQBO (SSW-EQBO) and eight during WQBO (SSW-WQBO). Several SSWs remained that did not belong to any of these groups and were disregarded. This is further justified because their associated vertical wind profiles corresponded to different transition phases, each one containing a very low number of cases so as to provide robust composites.

3. Isolation of the Tropical SSWs Signal

The downward propagation of the SSWs signal in the tropics can be analyzed by plotting time-height composites of SSW temperature anomalies in the tropical region, herein defined as the average from 10°S to 10°N. However, as stated in the section 1, the removal of the QBO signal in stratospheric temperatures is a major difficulty when characterizing the tropical cooling associated with SSWs. In this section, we test several methods to filter out the QBO from the SSWs composites. In a first attempt, anomalies are simply computed as deviations from the 34 year daily climatology. The resulting composite (Figure 2a) is shown from day −30 to day +30, considering day 0 as the central date defined in Table 1. The anomalous cooling starts 15 days before the SSW, and it peaks around day 0 at 10 hPa. The strongest cooling occurs in the upper levels and it weakens as it propagates downward, although a secondary minimum in temperature occurs at 70 hPa, 10–20 days after the central day. Figures 2b and 2c show the same SSW composite stratifying according with the QBO phase. Different from the case when all SSWs are considered (Figure 2a), during SSW-WQBO (Figure 2b), the largest anomalous cooling occurs around 20–40 hPa and persists until day +10 without reaching the lowermost stratosphere. The behavior of the SSW-EQBO (Figure 2c) reveals several differences with respect to SSW-WQBO. First, the cold anomalies at the upper levels persist during the 60 days, and reach the maximum at the central days. Second, an anomalous warming occurs between 20 and 40 hPa,

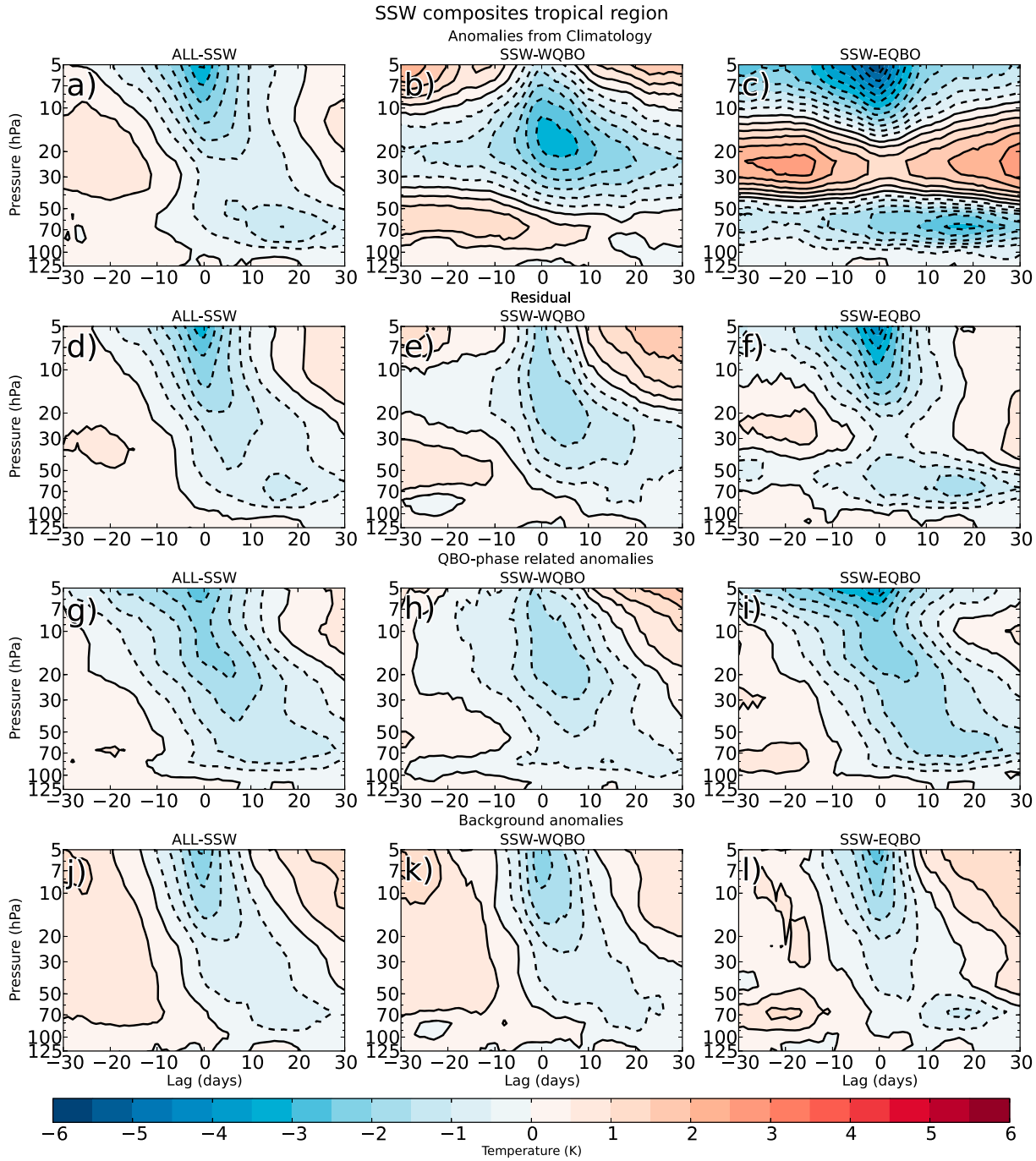

Figure 2. Pressure-time SSWs composites of the temperature in the tropical region (10°N–10°S) following different methodologies to remove the QBO influence on temperature by means of temperature anomalies with reference to the following: (a–c) full climatology , (d–f) a multiple linear regression, (g–i) a QBO-based climatology, and (j–l) the full climatology and a 61 day mean around the central dates. All four rows have three subplots for all (Figures 2a, 2d, 2g, and 2j), WQBO (Figures 2b, 2e, 2h, and 2k), and EQBO (Figures 2c, 2f, 2i, and 2l) SSWs. See text for details.

which weakens around day 0, in response to the cooling peak of the SSW (see Figure 1). Third, below this warm layer, anomalous cooling is observed from 50 to 100 hPa, being the largest between day 10 and 20.

The occurrence of these layers of opposite temperature anomalies in the SSW composites is related to the QBO imprint in tropical temperatures. According to the QBO definition adopted in section 2, EQBO (compared with WQBO) is overall warmer in the 20–40 hPa layer and colder in the 50–100 hPa layer, regardless

of the SSW occurrence (not shown). This is associated with the characteristic vertical wind profile of EQBO phases in tropical regions, which leads to positive wind shear (increasing westerly winds with increasing height) and warm temperatures between 10 and 50 hPa. The opposite situation occurs during the WQBO phase. Thus, the use of climatological anomalies to analyze the behavior of SSWs in the tropics mainly reflects the signature of the QBO phase. This methodology can also disturb the analysis of SSWs composites including all QBO phases (Figure 2a), because the unequal number of EQBO and WQBO winters influences the climatology. Therefore, we cannot assess whether or not the increased cooling in the lower stratosphere that appears in Figure 2a corresponds to the overweight of the SSW composite during EQBO with respect to those in WQBO or it is a signature characteristic of SSWs. This illustrates the need for a different methodology that removes the QBO signal and isolates the tropical response to SSWs. With this objective in mind, we have applied three different methods:

1. Residual composites: A multiple linear regression (MLR) has been performed to eliminate variability related to the annual and semiannual cycles, trends, volcanic eruptions, El Niño-Southern Oscillation, and QBO:

$$T(t) = a \cdot \sin(2\pi t/365) + b \cdot \cos(2\pi t/365) + c \cdot \sin(4\pi t/365) + d \cdot \cos(4\pi t/365)$$

$$+e \cdot t + f \cdot \mathrm{AOD}(t) + g \cdot \mathrm{N3.4}(t) + h \cdot U_{44.4\ \mathrm{hPa}} + i \cdot U_{9.9\ \mathrm{hPa}} + \zeta(t)$$

   where several indices have been used, including the first two harmonics for annual and semiannual variations, a linear fit, an atmospheric optical depth index for the volcanic influence (AOD), El Niño-Southern Oscillation 3.4 index (N3.4), and the two almost orthogonal indices: zonal mean zonal wind at 44 hPa and at 10 hPa for the QBO. Then, new SSW composites are computed using the residual of the MLR. Results are shown in Figures 2d–2f. The composite for all SSWs is similar to that using climatological anomalies (cf. Figures 2d and 2a). The SSW-EQBO and SSW-WQBO composites show a more clear downward propagation of the temperature pattern, but the layered temperature structure of Figures 2b and 2c still remains. Thus, although this technique does reduce the QBO signature, it does not remove it completely.
2. QBO phase-related anomalies: Anomalies are computed using a QBO-dependent climatology. For each day around the SSW date and each SSW, the climatology was computed from years without SSW in the ±30 day period around the central date and the same QBO phase as the given SSW. Results are shown in Figures 2g–2i. In this case, composites for the three subsets (All SSWs, SSW-WQBO, and SSW-EQBO) resemble those obtained with the MLR residuals (Figures 2d–2f), although the downward propagation is smoother when the climatologies take into account the QBO phase. However, ought to the small length of the database, some of these climatologies are computed based on only six winters, difficulting any robust statistical assessment.
3. Background anomalies: This method is based on *Kodera* [2006]. The seasonal cycle is removed together with the baseline state of each SSW, herein characterized by the 61 day mean around the central day (Figures 2j–2l). The three composites (All SSW, SSW-WQBO, and SSW-EQBO) are similar to each other, differing only in the speed of the downward propagation. For SSW-EQBO the maximum cooling descends to 30 hPa in about 2–3 days, faster than in the SSW-WQBO composite (about 8 days). However, the timing of the maximum cooling in the lower stratosphere is similar during both SSW-QBO phases. Although this is the method that reduces the QBO signatures the most, it requires an arbitrary offset (the 61 day mean around the central date), and the results depend on the number of days used to define the baseline state. Thus, for example, when considering a 41 day mean around the central date, the cold anomalies persist 18 days at 10 hPa (not shown), instead of the 24 days observed in Figure 2j. The sensitivity of the results to the length of the period employed to define the baseline state makes difficult to compute objective diagnostics of the SSW signal (e.g., persistence of the tropical cooling).

4. SSW Tropical Signal Propagation

Despite the differences and shortcomings of the aforementioned methodologies to characterize the SSWs evolution, all the signals share a tropical cooling accompanying the warming associated with the SSWs over the polar cap. This link between tropical and extratropical temperatures during SSWs can be quantified through the temperature anomalies around the SSWs. CP07 defined the SSW strength as the average of the anomalous temperatures over the polar cap (50°–90°N) for the 5 day period from the SSW's central date, which requires defining anomalies with respect to a daily climatology. Here we use their metric

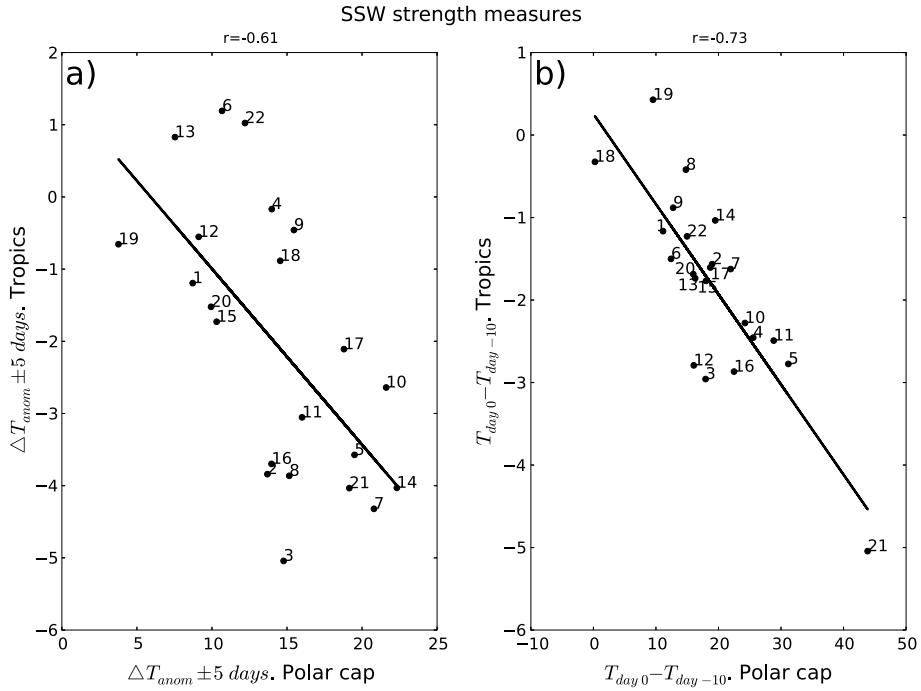

Figure 3. (a) Scatter plot of temperature anomaly at 9.9 hPa averaged for ±5 days from central date for polar (60°–90°N) versus tropical (10°N–10°S) regions. Numbers indicate the event on Table 1. The black line indicates the regression fit using least squares. (b) Same as Figure 3a but for temperature difference at 9.9 hPa between day 0 minus day −10.

referred to our new central dates and define the polar cap as the 60°–90°N region. Figure 3a shows the relationship between this benchmark (*x* axis) and the same measure applied to the tropics (10°N–10°S) (*y* axis). The Spearman correlation coefficient between the tropical and extratropical benchmarks is 0.61, statistically significant at the 95% significant level.

A stronger relationship between the responses in tropics and extratropics is found when the use of anomalies is partially avoided. To do so, we define the strength of the SSW as the temperature difference between day −10 and day 0 after removing the seasonal cycle (similar results are obtained if the seasonal cycle is not removed). This temperature difference is equivalent to an average of temperature tendency that is proportional to the meridional circulation $\left(\frac{\partial T}{\partial t} \approx N^2 w^*\right)$. Figure 3b shows the polar-tropical scatter plot of this new measure. There is a strong linear correlation between tropical and extratropical SSW signals, with a Spearman correlation coefficient of 0.75 (statistically significant at 99%). The fit of the data to the linear model is now improved, compared to that of Figure 3a. This improvement results in part from a better characterization of the SSW signal by avoiding the definition of a climatological mean state, biased by the QBO phase.

The results from Figure 3b suggest that this new metric (the relative temperature change) could also be more suitable to isolate the tropical cooling related to SSWs from the QBO temperature imprint. Thus, a new composite method is presented attempting to overcome the difficulties in isolating the SSWs tropical signal and to partially avoid arbitrary choices, as those presented in section 3. This novel methodology is based on the evolution of temperature differences with respect to the SSW central date, rather than on canonical anomalies relative to a mean state. First, the seasonal cycle is removed (although similar results are obtained if we use absolute values), and the central date of a given SSW is used as a temporal reference (day 0) for each pressure level. Thus, at each pressure level and each day around the central date, the signal is computed as the difference between the temperature values of that day and the central date. This provides the evolution of temperature around the central date (*x* axis) at different pressure levels (*y* axis). These evolution lines are then composited according to SSW-EQBO (blue) and SSW-WQBO (red) and shown in Figure 4b. Thin grey horizontal lines mark the reference value (temperature of day 0) at each level. Values above the

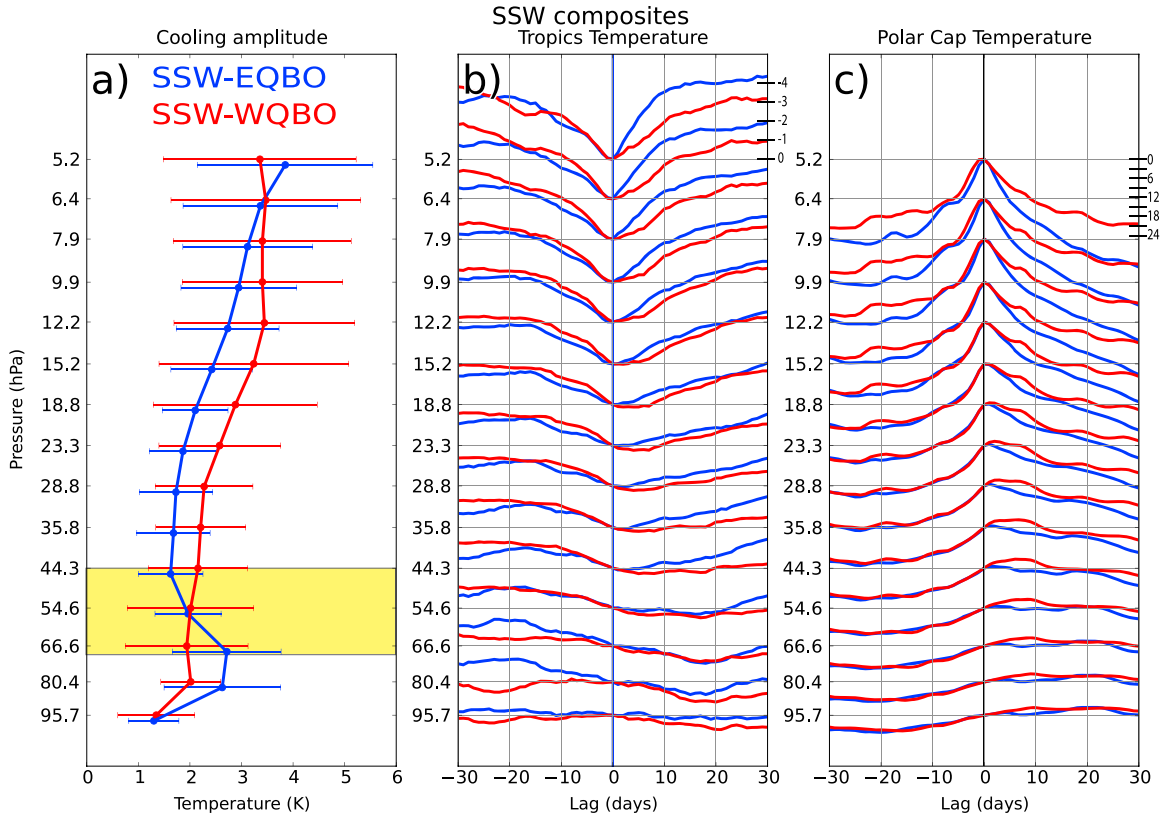

Figure 4. (a) SSW cooling amplitude at each pressure level, defined as the temperature difference between its maximum value, in the period day 0 to day −20, and its minimum value in the period day 0 to day +20. Error bars indicate ±1 standard deviation. Yellow region indicates statistical confidence at 90% level for the difference between the vertical grandient of cooling amplitude during both QBO phases. (b) SSWs composites of tropical temperature variations with respect to day 0 at each pressure level (marked by thin grey horizontal lines). (c) Same as Figure 4b but for the polar cap region. Blue for east and red for west QBO phases. The scales of temperature variations are indicated on the upper level. The scale ratio of polar versus tropical temperature is 6.

reference level imply cooling if the day is before day 0 and warming for days after day 0. Values below the reference level indicate warming before day 0 and cooling after it.

With this diagnostic, the possible QBO imprint in temperature at each level is filtered out as the QBO is expected to operate at longer time scales. The QBO has a period of around 28 months, and the QBO-related change in temperature is ∼3 K (varying with height) over 14 months, so the average tendency is ∼0.2 K/month. This temperature change is small compared to the changes observed in Figure 3. Thus, the temperature evolution at each level in Figure 4b can be attributed almost exclusively to SSWs. However, it is important to note that differences in the temperature evolution of the SSWs signal from one level to another are expected to be associated with the vertical structure of the background flow, which varies with height and it is different for each QBO phase. This will be discussed later.

Figure 4b provides the vertical structure of the SSW signal in the stratosphere and how it evolves with time. The results indicate a strong cooling during both phases of the QBO at each level, being the largest in the upper stratosphere. Below 10 hPa, the minimum temperatures during both QBO phases occur at progressively later times, lagging the central date of the SSWs by a few days. This reveals a downward propagation of the SSW-related cooling through the entire stratosphere (note the difference with, for example, Figure 2b, which suggested that the SSW signal does not reach the lowermost stratosphere during WQBO). Despite this common behavior, there are remarkable differences in the SSW propagation signal between QBO phases. Above 10 hPa, the cooling related to SSWs is short lived during EQBO as compared to SSW-WQBO cases. Furthermore, the strongest cooling below 10 hPa is more pronounced and occurs later during SSW-WQBO than during SSW-EQBO (e.g., at 23 hPa, the minimum temperature is reached around day 5 for SSW-WQBO and close to day 2 for SSW-EQBO). This behavior persists downward until 54 hPa, where the composite evolutions of SSWs signals during both QBO phases are comparable.

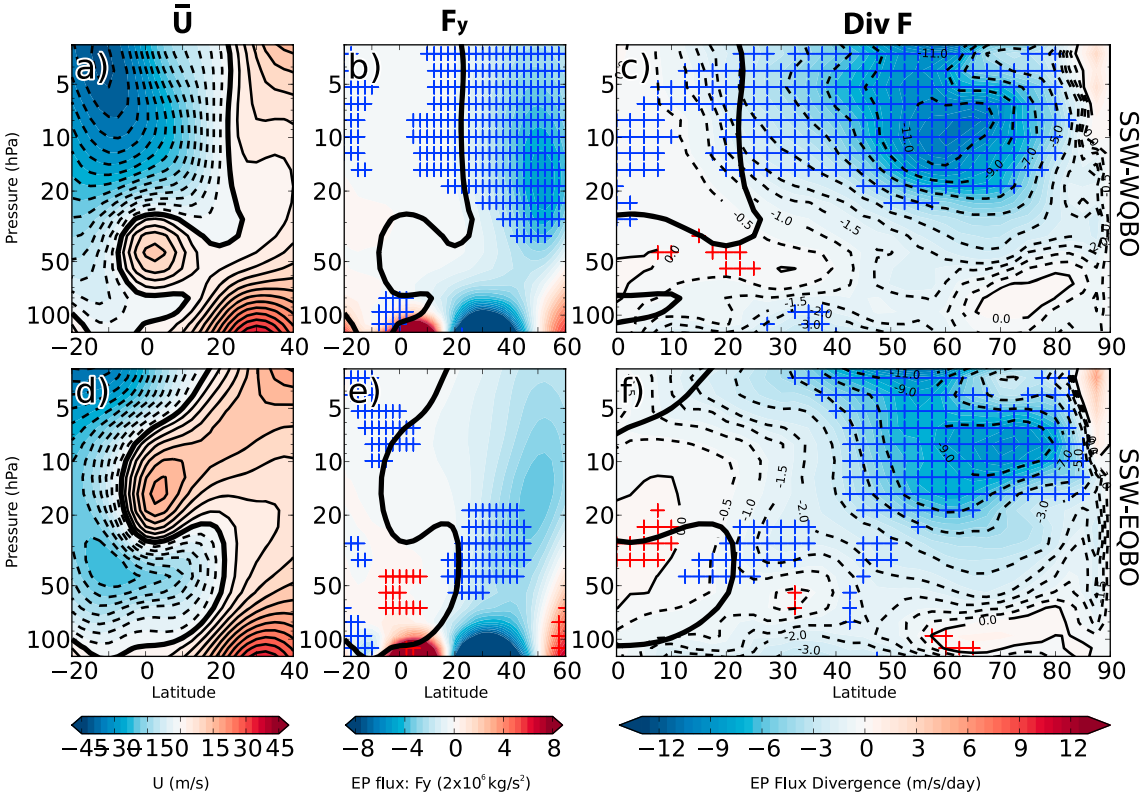

Figure 5. (a, d) SSWs cross-section composites of the zonal mean zonal wind average for ±30 days from central day during WQBO (Figure 5a) and EQBO (Figure 5d). (b, e) SSWs cross-section composites of the vertical component of the Eliassen-Palm (Fy) averaged for ±5 days from central day. Crosses indicate statistical confidence at 90% level of a Monte Carlo test taking random composites for their respective QBO phase subset of years, red crosses above 95th percentile and blue ones under 5th percentile. (c, f) Same as middle column but for Eliassen-Palm divergence.

Figure 3 indicated a close link between the tropical and polar cap (60°–90°N) temperature variations around the central date of SSW. Therefore, we next address whether the SSW signals over these two regions also exhibit a similar evolution. To do so, a composite analysis based on temperature changes was performed for the SSW signal over the polar cap (Figure 4c) in the same manner as in the tropical region. At high latitudes, the warming associated with SSWs above 44 hPa lasts longer during WQBO than during EQBO similar to the behavior of the tropics. This suggests that the temperature changes in the tropical stratosphere are coupled to the SSW temperature evolution over the polar cap. Below 44hPa, the temperature evolution in the tropics differs from that in the Northern Hemisphere (NH) high latitudes. This indicates that the march of the SSW signal in the tropical lower stratosphere is independent from that in the high latitudes, and hence, it should be related to mechanisms operating outside of the NH polar region.

In addition to the timing and persistence of the cooling associated with SSWs, it is also important to characterize the amplitude of the signal and its modulation by the QBO. As a measure of the SSW tropical cooling amplitude, we consider the temperature difference between the maximum value reached in the 20 days before day 0 and the minimum value reached in the period 0 to +20 day. This metric is computed for each event at each level, and then composited for SSWs according to their QBO phase (Figure 4a). Thus, positive values indicate an overall cooling around the SSW central date. A *t* Student test at the 90% confidence level has been performed to analyze the differences between both phases in the vertical gradient of this amplitude, in other words, if the cooling variation from one level to the next below differs among phases (yellow region). The SSW cooling is generally larger for SSWs occurring during WQBO (in red; note, however, the large case-to-case variability marked by the standard deviation bar). During SSW-WQBO, the cooling amplitude barely changes above 12 hPa while below this level, it decreases downward. Different from SSW-WQBO cases, the cooling amplitude during SSW-EQBO is the largest in the upper stratosphere and decreases progressively downward up to 44 hPa. However, this behavior reverses and the cooling enhances at lower levels (from 44 to 67 hPa), while it continues decreasing during SSW-WQBO cases. This cooling enhancement is

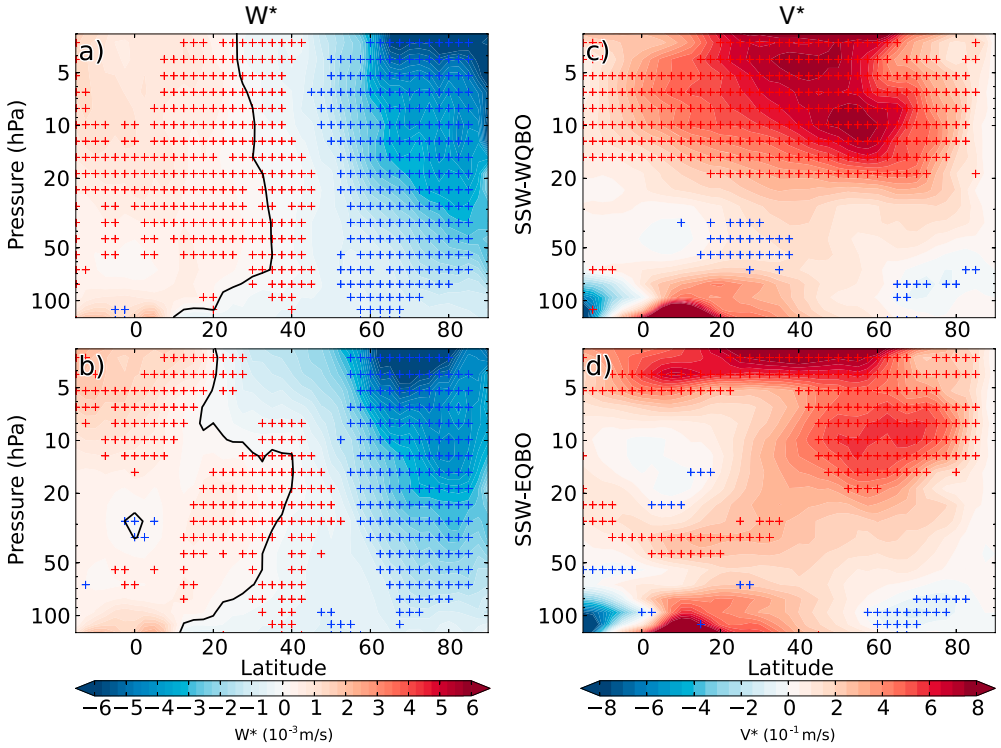

Figure 6. As in Figures 5b and 5e but for (a, b) vertical and (c, d) meridional residual circulation.

statistically different from the cooling weakening of SSW-WQBO at these levels (yellow region). In the lowermost tropical stratosphere (between 80 and 96 hPa), the temperature amplitude drops to small values for both QBO phases, indicating that the SSW tropical cooling signal weakens severely or disappears below 80 hPa. As it was argued above when analyzing the time evolution of the SSW cooling, the tropical signal in the midstratosphere seems to be tied to the polar region, with SSW-WQBO cases displaying a more persistent and pronounced cooling. This is in agreement with the behavior of the cooling amplitude in the tropics above 44 hPa level which exhibits a sustained cooling with height during SSW-WQBO events and a faster attenuation of the SSW cooling during EQBO. However, as stated before, such a coupling between tropical and extratropical regions does not appear below 44 hPa (see Figure 4), and hence, other mechanisms need to be operating in the lower stratosphere to explain the increase in cooling amplitude during SSW-EQBO.

To investigate this further, Figures 5a and 5d show composites of the zonal mean zonal wind for each SSW-QBO subset. The position of the zero-wind line, i.e., the change from westerlies to easterlies (thick black line in the figures) varies from WQBO to EQBO. This change modifies the equatorward propagation of planetary waves since they only propagate through a westerly background flow [*Charney and Drazin*, 1961]. The different QBO pathways for wave propagation are expected to also modulate the regions of wave dissipation which could ultimately alter the tropical upwelling below (downward control principle, *Haynes et al.* [1991]) and thus the tropical cooling during SSWs. To assess the differences in the preferred regions of wave dissipation between opposite SSW-QBO cases, Figures 5c and 5f display composites of the Eliassen-Palm (EP) flux divergence for SSWs occurring during both QBO phases for the ±5 days period. The statistically significance of these composites has been assessed through a 5000 trial Monte Carlo test. For each QBO phase, random composites of EP flux divergence were computed containing as many cases as SSWs were in each QBO subset. The cases in the random composites kept the day and the month of the observed SSWs, but the year of occurrence was chosen randomly among the available years of each analyzed QBO subset. Statistical confidence at the 90% level is attained when the EP flux divergence values are above the 95th (red crosses) or below the 5th (blue crosses) percentile of the probability distribution derived from the Monte Carlo distribution. Similar composites for the Eliassen-Palm meridional component, Fy, shown in Figures 5b and 5e indicate an increased wave propagation equatorward, in accordance with the different wave dissipation for both QBO phases during SSWs.

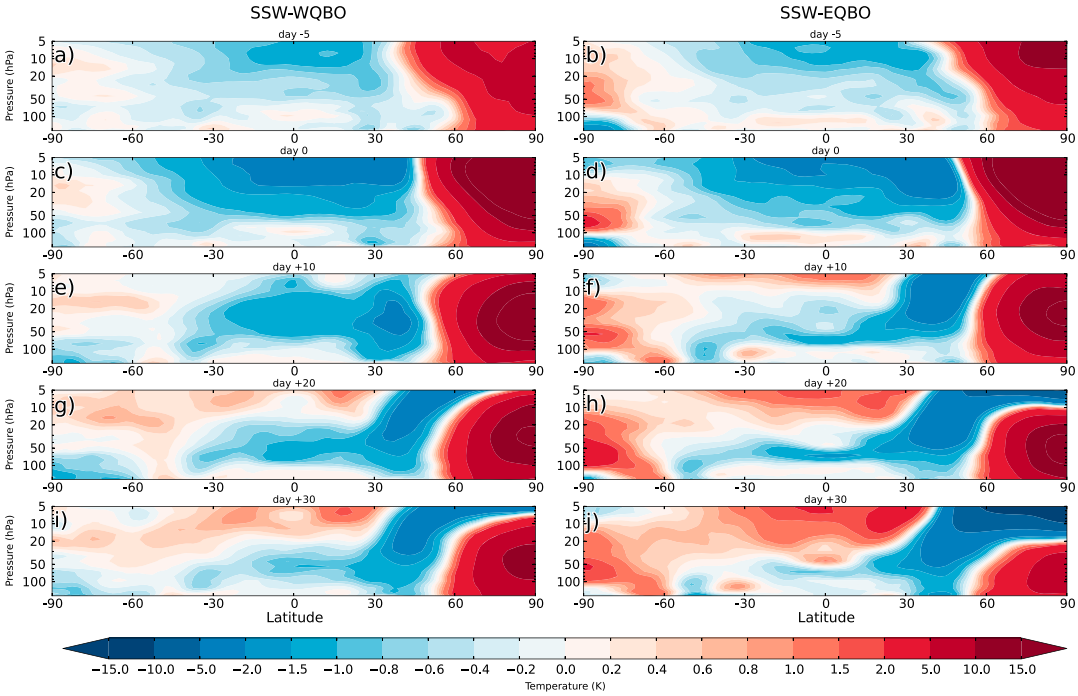

Figure 7. SSWs composites of the anomalies of the zonal mean temperature changes between the following: (a, b) day −5, (c, d) day 0, (e, f) day +10, (g, h) day +20, (i, j) day +30, and the averaged period from day −15 to day −10. For SSW-WQBO (Figures 7a, 7c, 7e, 7g, and 7i) and SSW-EQBO (Figures 7b, 7d, 7f, 7h, 7j).

Not surprisingly, during SSWs occurring in both QBO phases, there is EP flux convergence north of 15°N in the entire stratosphere, related to the large wave activity coming from the troposphere at midlatitudes in relation to SSWs [e.g., *McIntyre*, 1982; *Polvani and Waugh*, 2004]. However, differences between QBO phases do appear in the subtropics. Regions of significant convergence (enhanced dissipation), compared to their own QBO-based climatology, are observed above 15 hPa during SSW-WQBO and between 20 and 44 hPa for SSW-EQBO. These regions are well collocated with their respective QBO zero-wind lines at subtropical latitudes, reflecting their QBO dependency. According to the downward control principle [*Haynes et al.*, 1991], during SSW-EQBO, the subtropical convergence near 30 hPa intensifies the upwelling equatorward at lower levels and thus favors colder temperatures therein. Figure 6 shows composites for meridional and vertical residual velocities (v^*, w^*) in a similar way as Figures 5c and 5f for the ±5 days period. During SSW-WQBO more tropical upwelling occurs between 20 and 10 hPa (Figure 6a) accompanied with higher meridional circulation above (Figure 6c). Meanwhile, during SSW-EQBO, more equatorial upwelling is observed above 10 hPa and below 50 hPa, while lower upwelling than normal is observed around 30 hPa (Figure 6b). At the same time, the meridional residual velocity is higher between 50 and 30 hPa (Figure 6d), implying a secondary meridional circulation generated by the subtropical wave dissipation. This is consistent with the distinctive enhanced cooling amplitude observed in the lower stratosphere in SSW-EQBO (Figure 4a). Similarly, during SSW-WQBO, the SSW cooling amplitude in the upper levels (Figure 4a) does not decrease downward, as in the SSW-EQBO, but it is rather sustained with height, which agrees with the increased wave dissipation observed at those levels in Figure 5. Thus, differences in the subtropical wave dissipation associated with the QBO phase background state modulate the cooling amplitude in the tropical stratosphere in response to SSWs.

Up to this point, the tropical signal of SSWs and the differences between QBO phases have been analyzed for the averaged tropical region (10°N–10°S). We next address the latitudinal extension of the SSW signal and whether or not the aforementioned differences between EQBO and WQBO are confined to the equatorial region. Figure 7 depicts latitude-altitude composites of the anomalous zonal mean temperature changes for several days of the SSW's life cycle (-5, 0, +10, +20, and +30) relative to the averaged period between day −15 and day −10. The anomalies of the temperature variations are calculated subtracting the corresponding climatological temperature differences with respect to the calendar day of the given SSW. Figure 7 provides

a global picture of the temporal evolution of the SSW signal in the stratosphere. Note that negative values indicate an overall cooling from 15 to 10 days before the SSW to the indicated date.

These plots reveal a symmetric behavior of the SSW signal within the tropics relative to the equator that supports the tropical region chosen for our analysis (10°S to 10°N). The latitudinal belt of 15°–20° already displays some hemispheric asymmetries in the response to SSW, particularly for the period after day +10. The latitudinal extension of the SSW cooling reaches 30°S, as reported by *Taguchi* [2011], although asymmetries between the Northern and Southern Hemispheres are evident at these subtropical latitudes; the cooling is stronger and more persistent in the Northern Hemisphere. Figures 7 also allows for a detailed analysis of the evolution of the zonal mean temperature during SSWs. The temperature pattern at the upper levels and day 0 (Figure 7c and 7d) exhibits a tropical-extratropical dipole, with the extratropical warming associated with SSWs being accompanied by a cooling from 50°N to almost 50°S that supports the tight coupling between tropical and extratropical temperature variations in the upper stratosphere discussed before (Figures 3b and 4). As time progresses, the largest warming in the polar region is located at lower heights, and thus, the warming in the upper stratosphere weakens and it is replaced by a cooling anomaly [*Limpasuvan et al.*, 2004]. This downward propagation is faster during SSW-EQBO, as it was found in Figure 4. At low latitudes, the middle stratospheric cooling associated with SSWs also disappears in about 10–20 days, although it persists longer during WQBO than during EQBO (cf. Figures 7e and 7f), similar to what is observed in the polar cap and Figure 4. The SSW-EQBO pattern shows a faster downward propagation in terms of the minimum temperature evolution at the tropics. Although the tropical cooling in the lower stratosphere is already detected within a few days after the SSW during both QBO phases and is more persistent (still evident 30 days after the SSW) than at upper levels. Note however that the tropical cooling of the lower stratosphere is more pronounced during SSW-EQBO than during SSW-WQBO at day +20 (cf. Figures 7g and 7h), confirming again the results of Figure 4, although at days +30 the cooling is larger for SSW-WQBO.

5. Summary

In this study, ERA-Interim reanalysis data have been used to improve our understanding of the tropical signal associated with SSWs, with special focus on its evolution and behavior during different QBO phases. The removal of the QBO signal in stratospheric temperatures is a major difficulty when characterizing the evolution and downward propagation of the tropical cooling associated with SSWs. It has also been shown that composites of cross sections (days versus altitude) of SSW temperature anomalies show layers of alternating sign ought to QBO temperature imprints. Residual composites computed from a multilinear regression, and departures from a specific QBO-based climatology reduce these issues, although they do not eliminate completely the QBO signatures. Alternatively, the removal of a background state defined from an average period does a better job at isolating the SSW signal but depends on subjective choices as the length of the period.

We propose a new methodology based on the relative evolution of temperature at each level and a measure for the cooling amplitude. They provide a clearer characterization of the SSW signal and the differences in its propagation between QBO phases, avoiding the aforementioned problems. In addition, a measure of the SSWs strength has been proposed based on temperature differences from day 0 to day −10 at 10 hPa, which reflects a strong linear correlation of temperature variations between low and high latitudes.

The analysis based on temperature variations with respect to the central date of the SSW indicates that the SSW cooling in the tropical middle stratosphere is tied to the evolution of temperature over the polar cap, while the SSW signal in the lower stratosphere is partially disconnected from polar changes. Overall, the largest cooling associated with SSW in the tropics appears in the upper stratosphere, and weakens as it propagates downward. While the magnitude of the cooling keeps constant at the largest values across the upper stratosphere (above 10 hPa) for SSW-WQBO, the cooling weakens at lower heights and proceeds downward at a faster rate for SSW-EQBO. However, in the lower stratosphere, the cooling intensifies for SSW-EQBO, which is not observed in SSW-WQBO. This behavior cannot be related to the temperature changes in the polar region. Instead, the analysis of the background wind and EP flux in the subtropics reveals a QBO modulation of wave dissipation through changes in the position of the zero-wind line that can explain the observed behavior in the cooling amplitude in response to the SSWs, as explained below. The minimum temperature occurs on day 0 at the upper levels and later in time at lower levels, faster for

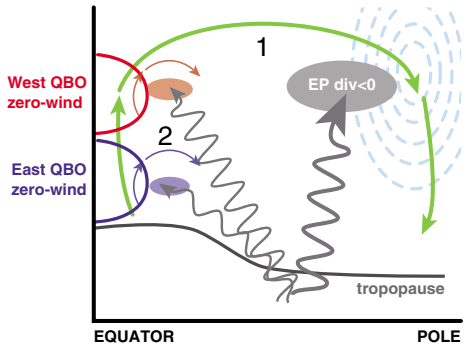

Figure 8. Scheme of the mechanisms for tropical stratospheric cooling associated with a SSW occurrence. The tropical region is affected by two pathways: (1) the increased residual mean circulation associated to the polar vortex break up and (2) the subtropical wave dissipation controlled by the position of the zero- wind line which in turn is modified by the QBO phase.

SSW-EQBO. In the lower stratosphere the temperature minimum is still remarkable more than 2 weeks after the central day. The temperature variations associated to the SSW are about 3 K at the upper levels, being larger around 10 hPa for SSW-WQBO than during SSW-EQBO. In the lower stratosphere from 44 hPa to 66.6 hPa, a temperature decrease of about 1 K occurs only for SSW-EQBO.

Thus, we propose two different pathways to explain the tropical temperature associated with SSW. They are summarized in the schematic of Figure 8. The first pathway strongly influences the SSW signal in the tropical upper stratosphere by changes in the mean meridional circulation that connect the tropical and polar regions (big green arrow). SSWs are triggered by enhanced wave activity at midlatitudes. Some of these waves dissipate at high latitudes and intensify the mean meridional circulation showing increased upwelling and cooling in the tropical region. This cooling occurs almost simultaneously with the polar cap warming and decreases as it propagates downward. The second pathway is related to the waves that propagate equatorward and whose dissipation can be modulated by the position of the zero-wind line, which depends on the QBO wind profile. This mechanism explains most of the differences observed in the tropical signal of SSWs between QBO phases. During WQBO, the zero-wind line is located above 30 hPa in the subtropics (red), and the increased wave activity during SSWs causes a region of enhanced wave dissipation and large cooling in the upper levels. This favors a vertically sustained cooling amplitude from 5 to 13 hPa. On the contrary, during SSW-EQBO, the largest EP flux divergence in the subtropics is located below 30 hPa (blue), in agreement with the zero-wind line position during EQBO, and consequently there is an enhanced cooling at the tropical lower stratosphere, in agreement with results from the temperature analysis. This second pathway occurs on the days close to day 0, so waves start to weaken the polar vortex first, and then also affect the subtropical region generating these secondary circulations and the extra tropical coolings apart from the generated by an increased mean residual circulation. These forcings of the stratospheric circulation at different levels could be related to different branches of the Brewer-Dobson circulation, to the upper and to the lower or shallow branch [*Plumb*, 2002].

These mechanisms have been found in reanalysis data. In a future study, we will investigate if they can be reproduced in long simulations of climate models, which can include many more SSW and thus reduce uncertainties. If this is the case, they could also be used as a potential diagnostic to validate performance of climate models in the stratosphere.

Acknowledgments
The authors want to thank three anonymous reviewers. This research was supported by the Ministry of Economy and Competitiveness of Spain under project TRODIM (CGL2007-65891-C02) and MATRES (CGL2012-34221). M.G.E. was funded by FPI grant (BES-2008-005310) and Consolider project (CSD 2007-00050).

References

Andrews, D. G., J. R. Holton, and C. B. Leovy (1987), *Middle Atmosphere Dynamics*, *Int. Geophys. Ser.*, vol. 40, Academic Press, San Diego, Calif.

Baldwin, M. P., et al. (2001), The quasi-biennial oscillation, *Rev. Geophys.*, *46*, 202–207.

Charlton, A. J., and L. M. Polvani (2007), A new look at stratospheric sudden warmings. Part I: Climatology and modeling benchmarks, *J. Clim.*, *20*, 449–469.

Charney, J. G., and P. G. Drazin (1961), Propagation of planetary-scale disturbances from the lower into the upper atmosphere, *J. Geophys. Res.*, *66*, 83–109.

Dee, D. P., et al. (2011), The ERA-Interim reanalysis: Configuration and performance of the data assimilation system, *Q. J. R. Meteorol. Soc.*, *137*, 553–597.

Haynes, P. H., M. E. McIntyre, T. G. Shepherd, C. J. Marks, and K. P. Shine (1991), On the downward control of extratropical diabatic circulations by eddy-induced mean zonal forces, *J. Atmos. Sci.*, *48*, 651–678.

Holton, J. R., and H. C. Tan (1980), The influence of the equatorial QBO in the global circulation at 50 mb, *J. Atmos. Sci.*, *37*, 2200–2208.

Holton, J., P. Haynes, M. E. McIntyre, A. Douglass, R. Rood, and L. Pfister (1995), Stratosphere-troposphere exchange, *Rev. Geophys.*, *33*, 403–439.

Kodera, K. (2006), Influence of stratospheric sudden warming on the equatorial troposphere, *Geophys. Res. Lett.*, *33*, L06804, doi:10.1029/2005GL024510.

Limpasuvan, V., D. W. J. Thompson, and D. L. Hartmann (2004), The life cycle of the Northern Hemisphere sudden stratospheric warmings, *J. Clim.*, *17*, 2584–2596.

Matsuno, T. (1971), A dynamical model of the stratospheric sudden warming, *J. Atmos. Sci.*, *28*, 1479–1494.

McIntyre, M. E. (1982), How well do we understand the dynamics of stratospheric warmings, *J. Meteorol. Soc. Jpn.*, *60*, 37–65.

Naito, Y., M. Taguchi, and S. Yoden (2003), A parameter sweep experiment on the effects of the equatorial QBO on stratospheric sudden warming events, *J. Atmos. Sci.*, *60*, 1380–1394.

Plumb, R. A. (2002), Stratospheric transport, *J. Meteorol. Soc. Jpn.*, *80*, 793–809.

Polvani, L. M., and D. W. Waugh (2004), Upward wave activity flux as a precursor to extreme stratospheric events and subsequent anomalous surface weather regimes, *J. Clim.*, *17*, 3548–3554.

Randel, W. J., R. R. Garcia, and F. Wu (2002), Time-dependent upwelling in the tropical lower stratosphere estimated from the zonal-mean momentum budget, *J. Atmos. Sci.*, *59*, 2141–2152.

Seviour, W. J. M., N. Butchart, and S. C. Hardiman (2012), The Brewer-Dobson circulation inferred from ERA-Interim, *Q. J. R. Meteorol. Soc.*, *138*, 878–888.

Taguchi, M. (2011), Latitudinal extension of cooling and upwelling signals associated with stratospheric sudden warmings, *J. Meteorol. Soc. Jpn.*, *89*, 571–580.

Yoshida, K., and K. Yamazaki (2011), Tropical cooling in the case of stratospheric sudden warming in January 2009: Focus on the tropical tropopause layer, *Atmos. Chem. Phys.*, *11*, 6325–6336.